Layer-selective spectroscopy of Fe/GaAs(001): Influence of the interface on the magnetic properties

L. Giovanelli,[1,2] G. Panaccione,[1] G. Rossi,[1,3] M. Fabrizioli,[1,4] C.-S. Tian,[5] P. L. Gastelois,[6] J. Fujii,[1] and C. H. Back[7]
[1]*INFM, TASC Laboratory, Area Science Park, S.S.14, Km 163.5, I-34012 Trieste, Italy*
[2]*L2MP-UMR CNRS 6137, Faculté des Sciences de Saint Jérôme, Case 142, 13397 Marseille Cedex 20, France*
[3]*INFM- Dipartimento di Fisica, Università di Modena e Reggio Emilia, Via A. Campi 213/A, I-41100 Modena, Italy*
[4]*Università degli Studi di Trieste, Piazzale Europa 1, I-34100 Trieste, Italy*
[5]*Physics Department, Fudan University, 200433 Shanghai, China*
[6]*CDTN/CNEN, Caixa Postale 941, 30123-970 Belo Horizonte, Minas Gerais, Brazil*
[7]*Institut fur Experimentelle Physik, Univ. Regensburg, D-93040 Regensburg, Germany*
(Received 4 February 2005; revised manuscript received 28 April 2005; published 25 July 2005)

We present magneto-optic Kerr effect, x-ray photoelectron spectroscopy, and x-ray magnetic circular dichroism data from epitaxial thin ferromagnetic film grown onto GaAs(001)-(4×6). By seeding a half monolayer of Co in an Fe double wedge with a total thickness of six monolayers, we introduced a *magnetic marker*, which, similarly to Mössbauer spectroscopy, allows us to probe the magnetic and chemical properties across the ferromagnetic film in a layer-dependent analysis. The long-range magnetization is found to persist within the Fe overlayer at any depth, until a reduction is observed at the interface with GaAs. Correspondingly the spin magnetic moment is maximum at the center of the film and is reduced both at the interface and at the surface. We found also an enhancement of the orbital magnetic moment and orbit-to-spin magnetic-moment ratio near the interface with the GaAs substrate. Further, an uneven segregation (diffusion) between Ga and As has been found, and its influence on magnetic properties is discussed.

DOI: 10.1103/PhysRevB.72.045221 PACS number(s): 75.70.Cn, 72.25.Mk, 75.60.−d, 79.60.−i

I. INTRODUCTION

The advances obtained over the last decade in magnetic storage technology are deeply connected with the properties of ferromagnetic thin films, and a great number of studies have been devoted to the comprehension of device structures based on ferromagnet (FM)/semiconductor (SC) interfaces; these hybrid systems display peculiar characteristics, such as giant magnetoresistance, complex magnetic anisotropy effects, and enhanced values of spin and orbital magnetic moments.

Among the possible procedures of thin film preparation, molecular beam epitaxy enables the best control of the parameters playing a key role for the magnetic and electronic properties, particularly when the delicate interplay between these properties originates at the interface between the FM film and the SC substrate. Growth of Fe on GaAs(100) represents a paradigmatic case: epitaxial conditions are easily matched in Fe/GaAs (001), due to the small mismatch (1.4%) between the bcc Fe lattice parameter and half the GaAs one.[2] Hence, Fe on GaAs has attracted strong interest, mainly motivated by the search for spin-injection devices. Indeed, the results from a magnetic and structural point of view have been very encouraging and spin injection efficiency up to 32% has been reported.[3] However, it was soon realized that not only the interfacial effects are of primary importance, but also that both substrate preparation conditions (temperature, surface reconstruction, termination of the surface) and growth mode strongly influence the Fe magnetic properties at the early stage of the interface formation.

The structural and magnetic properties of the Fe/GaAs(001)-(4×6) interface have been studied intensively by a number of experimental techniques[1–10] and theoretical calculations.[11–13] Fe films grow through islands formation up to ~3 monolayers (ML). At that coverage, the islands start coalescing in a corrugated layer with a bcc crystal structure and the ferromagnetic state sets in.[5] The Curie temperature increases for increasing film thickness and reaches room temperature at coverage of about 3.5 ML. On the other hand, the evolution of the ferromagnetic behavior as a function of Fe thickness is intimately connected with the presence of a in-plane uniaxial magnetic anisotropy (UMA): in the FM state, two nonequivalent high-symmetry directions cohabit, i.e., the [110] and [1 -1 0] of the (001) bcc Fe surface.[4–6,8–10] The easy axis along the [110] is very soft with a coercive field of about 20 Oe, whereas the perpendicular [1 -1 0] direction is an intermediate one with a saturation field of 1 kOe.[4–6,8,9] The two directions become almost equivalent for higher thicknesses. In fact, starting from about 20 ML, the expected cubic magnetic anisotropy is found with the easy axis along the Fe [100] directions.[6] Several scenarios have been proposed to explain the UMA behavior described above, ranging from anisotropic interface bonding to magneto-elastic coupling. Some recent theoretical[13,14] and experimental studies[15,16] have suggested that the former is more likely to be responsible for the observed phenomenon.

Furthermore, the presence of a magnetically dead layer at the interface between the two materials has been a question of debate in the past: the presence of such a "quenched" layer was suggested by Krebbs *et al.* to explain the decrease of the average magnetization value as a function of Fe film thickness.[17] The authors invoked different causes, as (i) the presence of a "magnetization dilution" due to thickness-dependent lattice compression (in order to relax the interface

mismatch), and (ii) the substrate atoms segregation and the formation of antiferromagnetic Fe_2As microcrystals. Recently, Claydon *et al.*, by using x-ray magnetic circular dichroism (XMCD) on capped samples, reported the absence of an Fe dead layer at the interface, with an Fe magnetic moment similar to the bulk value, and the enhancement of the Fe orbital moment at the interface.[18] Concerning Ga and As segregation, different mechanisms for the two materials have been put forward: As segregation is driven by the chemical bonding with Fe atoms, calculations propose that segregation of As takes place even at 0 K and accumulates at the Fe film surface; Ga segregates dynamically and deposits across the whole Fe film thickness.[13] It must be pointed out that the amount of film dilution by substrate segregation and its possible influence on the magnetic properties is an important ingredient when evaluating the feasibility of spin-injection devices based on the Fe/GaAs (001), in particular when considering that the working temperature of a real device will exceed room temperature. Nevertheless, in most of the experimental studies reports, the interplay between the chemical evolution of the interface and the magnetic properties has not been studied. This is mainly due to experimental difficulties (i) to avoid corrosion, in most cases capped samples have to be studied, and (ii) to obtain useful information, both element sensitivity and layer-dependent magnetic information across the interface are of crucial importance.

This study stems from the requirements of a thorough spectroscopic and magnetic analysis performed on samples prepared *in situ* under UHV conditions, thus avoiding the uncertainties introduced by capped samples. We present the magneto-optical Kerr effect (MOKE), x-ray photoelectron spectroscopy (XPS), and x-ray magnetic circular dichroism (XMCD) measurements, where we were able to probe the Fe magnetic properties along with the ferromagnetic film thickness, in a layer-dependent analysis. The central idea of this work was to exploit the characteristics of synchrotron radiation in a procedure similar to Mössbauer spectroscopy. By seeding half a monolayer (ML) of Co in a 6-ML film of Fe on GaAs(001)-(4×6), we introduced a *magnetic marker* that allows the careful monitoring of the magnetic properties of the Fe film as a function of the distance from the FM/SC interface, keeping unchanged the magnetic environment of the interface. The measured evolution of spin and orbital moment across the ferromagnetic film shows an enhancement of the orbital moment near the interface with GaAs, as well as a general decrease of the averaged magnetization when approaching the interface and at the film surface. Furthermore, XPS data clearly reveal that the diffusion of Ga and As is uneven through the magnetic layer, and that the layer-by-layer analysis of the magnetic signal does not reveal a magnetically quenched interface, even in the presence of Ga-Fe and As-Fe hybridization.

The paper is organized as follows: Sec. II describes the experimental setup and the procedure to prepare the samples, in Sec. III experimental results are presented, and Sec. IV is dedicated to the discussion.

II. EXPERIMENT

Experiments were performed at the advanced photoemission experiment (APE) beamline at the ELETTRA synchrotron radiation facility in Trieste.[19] The APE High energy (APE-HE) beamline delivers a high-flux, variable-polarization focalized photon beam with photon energy ranging from 150 to 1600 eV and with a resolving power of 7000 at 400 eV. The detection system consists of an Omicron EA125 electron energy analyzer for XPS, and a total yield channeltron electron multiplier for XMCD. The experimental setup includes a preparation chamber connected to the APE-HE end station through a transfer system in UHV. The preparation chamber at the APE beamline represents itself as a complete tool for surface analysis and thin-film magnetometry. The apparatus is equipped with a retarding field grid analyzer for structural and chemical analysis of the sample surface through low-energy electron diffraction (LEED), Auger electron spectroscopy (AES), and MOKE, with transverse, polar, and longitudinal geometry. Epitaxial growth was performed under UHV conditions by means of electron bombardment evaporators, a quartz balance for the film thickness calibration, and a shutter that could be placed in front of the sample to deposit films with variable thickness. The GaAs(001) substrates was cleaned in UHV (base vacuum 6×10^{-11} mbar) by cycles of sputtering (Ar^+, 1 keV) and annealing, after removal of the native oxide by flash annealing at 850 K. Sputtering for 1 h at a temperature of 900 K followed by a final annealing at 920 K resulted in a sharp 4×6 reconstruction as observed by LEED. Subsequently, Fe and Co were deposited at 5×10^{-10} mbar. The choice of coevaporation of Fe and Co is twofold: (i) $Fe_{50}Co_{50}$/GaAs (001) has an identical lattice parameter as Fe/GaAs (001), different from other possible Fe_xCo_{1-x} compositions;[20] (ii) the magnetic properties of the thin film are almost unperturbed by the presence of Co.[21] We prepared double wedges as sketched in Fig. 1. The procedure to prepare the composite films was the following: (a) a thin wedge-shaped layer of Fe was deposited on a freshly prepared GaAs(001)-(4×6) substrate. The thickness ranged from 0 to 6 ML over a sample length of 6 mm along the [110] easy magnetization direction. A small area of 1 mm was left uncovered near the edge of the sample. The wedge was obtained by progressively hiding the sample surface behind a shutter. (b) On this wedge a single monolayer of $Fe_{0.5}Co_{0.5}$ was deposited by coevaporation at a 0.4 ML/min rate from two adjacent sources in order to obtain a constant thickness of half a monolayer of Co placed at variable distances from the GaAs(001) surface. On the side of the sample left bare after the first evaporation, the 0.5 ML of Co atoms was in direct contact with the substrate. (c) A second wedge with opposite orientation was deposited. Also in this case, the first mm at the thick side of the first wedge was left uncovered by the second deposition so that on one side the Co half-monolayer was sitting on a 6-ML-thick Fe film without any further Fe capping.

As shown in Fig. 1, this procedures results in Co atoms embedded in an evenly thick 6-ML Fe film. The Co atoms reside at variable distances from the interface, acting as a magnetic marker along the film thickness. Typically a rate of 0.2 ML/min and a final thickness of 6 ML corresponds to 0.2 mm/min of movement, so that the 6-mm area was covered by a uniform wedge ranging from 0 to 6 ML, with a constant steepness of 1 ML/mm. After each stage of the film

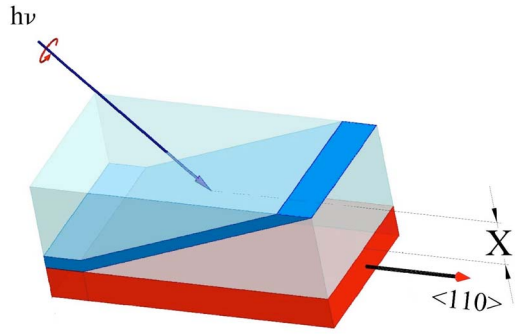

FIG. 1. (Color online) The cartoon of the sample and experimental geometry. The double-wedge structure consists of (i) an Fe wedge ranging from 0 to 6 ML deposited on the GaAs(001)-(4 $\times$6) and covering 6 out of 7 mm of the total substrate length; (ii) a single layer of $Fe_{0.5}Co_{0.5}$ covering the whole sample length; (iii) a 6-ML-thick Fe wedge oppositely oriented. The sample was remnantly magnetized in plane along the [110] direction. The x rays run parallel to the (1 -1 0) plane forming an angle of 45° with the sample magnetization. Scanning the sample along the [110] direction keeping fixed the x-ray beam resulted in probing Co atoms lying at variable distances from the interface with GaAs. This distance is referred as X in the paper. The x-rays were polarized, respectively, circularly and linearly (along the [1 -1 0] direction) for XMCD and XPS measurements.

preparation, the sample was studied by LEED and MOKE. The electron beam of the retarding grid analyzer and the laser beam used in MOKE have a section size of less than 0.5 mm. Impinging with the focused beam onto different regions of the sample surface, we were thus able to probe the structural and magnetic properties along the wedge(s), e.g., to check the onset of ferromagnetism and its relation with the presence of a bcc structure as a function of film thickness in the first deposited wedge. From the preparation chamber, the samples can be transferred in UHV to the end station.

Core level (CL) photoemission was performed at room temperature (RT), in normal incidence, and 45° off-normal emission using in-plane, linearly polarized x-rays at $h\nu$ =450 eV. Overall energy resolution (photons + analyzer) was set to $\approx$200 meV. X-ray absorption measurements and XMCD on Co and Fe $L_{2,3}$ edges were performed by switching circularly polarized light, with an energy resolution of $\approx$150 meV. In both photoemission and photoabsorption measurements, the x-ray beam size on the sample surface was of the order of 100 μm$\times$200 μm; the sample was moved in a direction perpendicular to the radiation direction to impinge with x rays on regions with different thicknesses (in the case of the simple wedge) or regions in which the Co atoms were sitting at different distances from the interface (in the case of the Co sandwiched between the two Fe wedges). The distance of the probed region from the interface is referred to as X in the rest of the paper (see Fig. 1). The complete analysis of the sample at each stage of preparation lasted about 5 h.

III. RESULTS

A. MOKE and LEED

In situ transverse MOKE loops were performed at RT on freshly prepared samples. The [110] direction was set perpendicular to the scattering plane in order to probe the magnetization along the easy axis of the UMA. Figures 2(a) and 2(b) present the result of the analysis of the Kerr signals recorded on the three subsequent steps (a), (b), and (c) of the double-wedge preparation described in Sec. II; the curves correspond to the Kerr signals measured at different positions of the sample, the x axis corresponding to the position of the Co marker layer with respect to the GaAs substrate. The Kerr loops were measured by shining the focused laser light at different positions of the sample, both in the case of the single wedges (bare and covered with 1 ML of $Fe_{0.5}Co_{0.5}$) and the double wedge; in the case of the single wedges, one probes Fe layers of increasing thicknesses. Figure 2(a) shows the remnant Kerr response (that in a first approximation is proportional to the net magnetization in zero field) for the three samples (a), (b), and (c), as mentioned in Sec. II. In agreement with previous studies performed on Fe/GaAs(001)-(4$\times$6), the FM state at RT sets in at 3$\pm$0.5 ML;[4,5] moreover, the remnant magnetization increases for increasing thickness as a larger amount of Fe atoms are probed. We remind that the critical FM thickness strongly depends on the substrate preparation and growth conditions.[4] When 1 ML of $Fe_{0.5}Co_{0.5}$ is added to the first Fe wedge, the critical thickness for the FM states increases only slightly and the hysteresis loop opens up at the overall thickness of about 3.2$\pm$0.5 ML. Consequently, the Kerr response at a given point of the sample is enhanced with respect to the

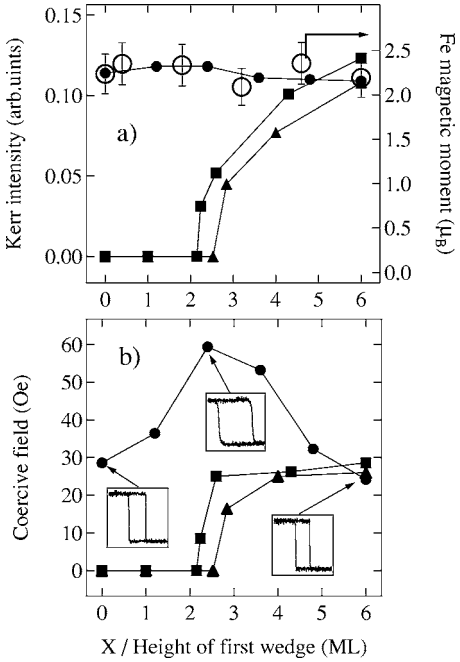

FIG. 2. The Kerr analysis results. (a) On the left axis the Kerr intensity (saturation magnetization) is plotted as a function of thickness for the wedge samples (triangles for the Fe wedge, squares for the Fe wedge covered with the $Fe_{0.5}Co_{0.5}$ ML) and as a function of X (see Fig. 1) for the double-wedge sample (filled circles). On the right axis the hollow circles represent the Fe magnetic moment at different X as measured by XMCD. (b) The coercive field H_c as a function of thickness for the wedge samples and X for the double-wedge sample [the symbol code is the same as in (a)].

simple Fe wedge. Finally, the sample magnetization results were constant across the whole sample in the case of the double-wedge sample. In Fig. 2(a) the Fe total magnetic moment measured by XMCD (see Sec. III) is plotted, revealing a good agreement with Kerr data.

Figure 2(b) shows the coercive field H_c values measured at different positions of the samples. For the two wedge-shaped samples, $H_c > 0$ at the onset of the FM state and it rapidly saturates at the maximum value of about 25 Oe. On the other hand, the double-wedge sample shows an increase of H_c in the central part of the sample. The insets show the magnetic hysteresis loops at selected positions along the double-wedge sample. LEED patterns were also measured at different thickness and, coherently with previous results,[4–6] the substrate diffraction pattern disappeared at the thinnest Fe coverage while a square pattern appeared at nominal thickness of 3 ML, displaying the 1×1 pattern of the bcc Fe(001). LEED measurements did not show any sizable difference after the deposition of 1 ML $Fe_{0.5}Co_{0.5}$ and/or in the double-wedge sample.

B. XPS

The chemical composition of the sample and its evolution as a function of steps (a), (b), and (c) to produce the double wedge was studied by XPS with synchrotron radiation. XPS is a surface-sensitive technique; therefore, by focusing the x-ray beam onto different regions of the sample, the chemical composition of the sample surface for different Fe thicknesses as well as the distance from the sample surface of the sensing Co layer was monitored measuring the intensity attenuation of the core levels. In Fig. 3(a) we show the XPS spectra of an Fe wedge deposited on freshly prepared GaAs(001)-(4×6). The nominal film thickness ranged from 0 to 6 ML as calibrated by the quartz balance thickness monitor. The topmost spectrum refers to a region of clean, uncovered GaAs(001)-(4×6); from top to bottom, spectra corresponding to regions with increasing thickness of Fe are shown. The acquisition time for the complete data set was 1 h. In the spectrum of clean GaAs(001)-(4×6), the valence band and both the Ga and As 3*d* core levels are clearly visible, respectively, at 430 eV and 408 eV of kinetic energy, together with the relative plasmon losses at about 15 eV higher binding energy (BE). As the Fe thickness increases, the growing intensity of Fe 3*p* core levels located at 396 eV and Fe 3*d* valence band are accompanied by the reduction of the Ga and As related peaks. The Fe 3*p* peak has a constant BE all through the series of spectra. On the other hand, the core levels of the substrate atoms show a progressive shift to lower the BE for increasing Fe thickness. This shift is small for the As 3*d* levels ($\approx$0.15 eV) and more pronounced for the Ga 3*d* core level, reaching a maximum of $\approx$0.8 eV. Figure 3(b) shows the same sample after the deposition of 1 ML of $Fe_{50}Co_{50}$. The line shapes are practically unaffected, except for a slight reduction of Ga and As peaks compared to the Fe one; Co 3*p* core levels appear at 392 eV, i.e., 4 eV higher BE with respect to Fe 3*p*. Figure 3(c) presents the spectra for the complete double-wedge sample where we observe that the Fe, As, and Ga features are rather constant in

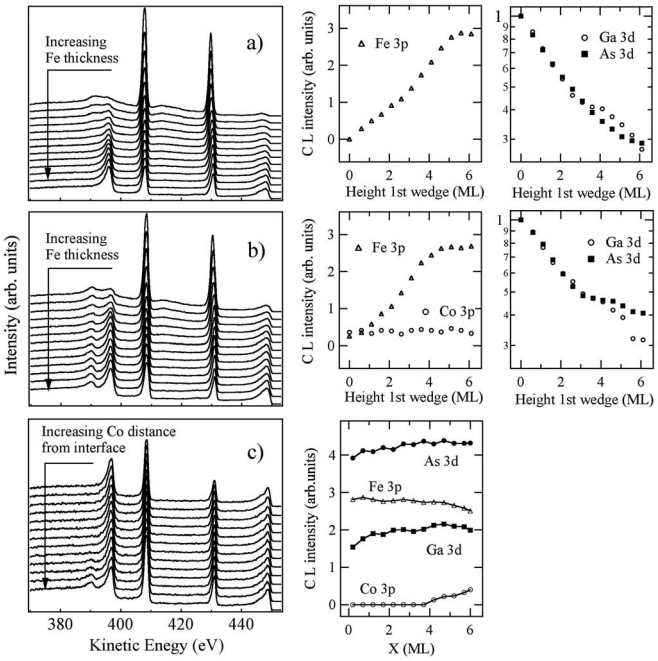

FIG. 3. Left panels: the XPS spectra taken at different position on the sample of (a) the Fe wedge, the upper spectrum corresponds to the bare GaAs(001)-(4×6) substrate; (b) the Fe wedge covered with 1 ML $Fe_{0.5}Co_{0.5}$; (c) the double-wedge sample, the upper spectra correspond to the to the region of the sample in which the Co atoms are in direct contact with the substrate. Right panels: the upper and middle panels represent the core level intensity corresponding to increasing film thickness. The substrate core-level intensities are normalized to the values of the bare substrate. The right lower panel represents the double-wedge core levels along the sample length.

intensity while there is an increase of the Co 3*p* peak only at one side of the sample.

The intensities of the As 3*d*, Ga 3*d*, Fe 3*p*, and Co 3*p* core levels are presented as side panels in Fig. 3 for the corresponding samples. In the right panel of Fig. 3(a) the Ga and As 3*d* peak intensities normalized to the ones of the clean sample are plotted on a logarithmic scale. The attenuation of the substrate signal follows an exponential behavior up to a nominal coverage of $\approx$3 ML. For coverage between 3 and 4 ML, the Ga-related intensity decreases less rapidly than the As one and, finally, this tendency is inverted for higher coverage. The intensity of the Fe 3*p* peak increases almost linearly up to about 3 ML coverage, then a sudden change is found in the growing trend. It is interesting to note that this thickness corresponds to the coalescence of Fe islands. Once the single layer of $Fe_{0.5}Co_{0.5}$ is deposited over the Fe wedge, the Co 3*p* core levels appear as a feature at the high BE side of the Fe 3*p* levels. The Co 3*p* intensity is constant through the whole wedge, suggesting that the diffusion of Co atoms into the Fe film is negligible. The Fe 3*p* core levels increase in intensity similarly to what was found for the simple Fe wedge and the same holds for the Ga and As features, although the As-to-Ga ratio increases on the thick side of the sample.

The analysis of the double-wedge sample is presented in Fig. 3(c). The intensity of the Fe 3*p*, Ga 3*d*, and As 3*d* levels

is constant within the error expected from the XPS thickness analysis. An evaluation of the film thickness variation through the core level intensities shows that there is an increase of the Fe film height $\leqslant 15\%$ between the two edges of the sample. For what concerns Co $3p$, a sizable signal is found only within 2.5 ML from the surface, as expected when considering the attenuation of the Fe counterwedge.

C. XMCD

The double-wedge samples, magnetized in plane, were measured at 45° with respect to the light propagation direction. The Co $L_{2,3}$ absorption edges were measured in total electron yield mode by collecting the secondary electrons with a channeltron placed above the sample. XMCD spectra were obtained by flipping the circularly polarized radiation, scanning the sample along the easy axis direction with steps of about 0.5 mm. Given the double-wedge geometry, this step entails probe regions with Co atoms at different distances from the FM/SC interface, at steps of 0.7 ML within the Fe film. Since no appreciable diffusion of the Co atoms was detected by XPS, the error bar of the probing depth can be confidently assigned within the portion of the Co probe enlightened by the x-ray beam, i.e., ~ 300 μm or 0.3 ML. In Fig. 4 we show three representative XMCD spectra, corresponding to 4.6, 1.8, and 0.4 ML from the GaAs substrate. The spectra have been normalized to the incident photon flux as measured on a calibrated photodiode. Although all three spectra display nonzero dichroism, their intensity at the L_3 and L_2 edges differs significantly as a function of the distance from the interface. Since the samples are magnetized, the asymmetry at L_3—i.e., the dichroic signal normalized to the total absorption cross section—can be considered as proportional to the local magnetization.[23–27] Figure 5(a) summarizes the values of the asymmetry measured at the Co L_3 edge vs the Co position along the double wedge. We observe the presence of a net dichroic signal through the whole interface, including the case of Co atoms in direct contact with the GaAs substrate. The asymmetry is higher in the center of the layer and it is reduced both near the interface and near the surface.

The capability of XMCD to probe the magnetic properties of composite materials in a chemically sensitive way goes beyond the chemically sensitive magnetometry. Making use of the magneto-optical sum rules, it is possible to measure separately the orbital and spin moment expectation values on a per-atom base[24,28]

$$m_{orb} = \frac{2}{3}\frac{\Delta_3 + \Delta_2}{I_{iso}}(10 - n_{3d}), \tag{1}$$

$$m_{spin} + \frac{7}{2}m_T = \frac{\Delta_3 - 2\Delta_2}{I_{iso}}(10 - n_{3d}), \tag{2}$$

where Δ_3 and Δ_2 are the areas of the dichroic spectrum relative to the L_3 and L_2 spin-orbit split edges transitions corrected for the incomplete circular polarization and I_{iso} is the total area under the isotropic spectrum (i.e., the average between spectra taken with opposite polarization) after background subtraction. n_{3d} is the number of electrons in the Co $3d$ band. We set this value equal to 1.62 as reported in a previous study for a thick FeCo film.[29] $m_{spin}^{eff} = m_{spin} + 7/2 m_T$ represents the isotropic spin magnetic moment corrected by the magnetic dipole term.[28] As pointed out in Ref. 24, due to the high symmetry of the atomic environment, this last term is expected to have minor influence with respect to the effective spin moment. In Figs. 5(b)–5(d) the values of m_{orb}, m_{spin}^{eff}, and their ratio as a function of the distance X from the interface are presented. In the figures, we report for comparison the values corresponding to an hcp thick film[24] (dashed line) and those measured for a thick FeCo film, that is, $m_{orb} = 0.173\mu_B, m_{spin}^{eff} = 1.48\mu_B$ (continuous line, our data). The Co spin magnetic moment through the entire film is sensibly lower than that of a thick hcp film and it is reduced also with respect to the bcc FeCo film. Nevertheless it is quite close to the value of $1.44\mu_B$ found in a recent XMCD study performed on a 36-Å-thick bcc Co film on Ge(100).[30]

The behavior of the spin magnetic moment within the 6-ML film shows a reduction in proximity of the interface and at the surface of the sample. The orbital magnetic moment is instead—on the average—aligned with reference values, but its layer dependence shows a noticeable augmenta-

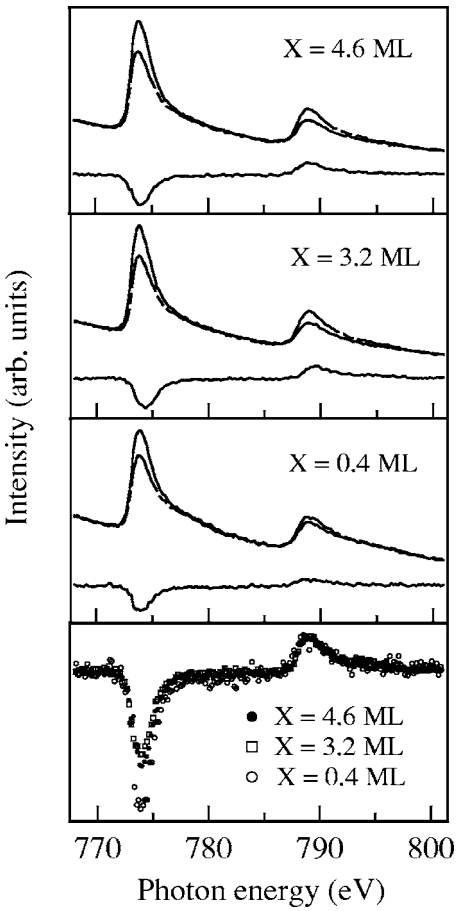

FIG. 4. XMCD results. Upper panels: Co $L_{2,3}$ XMCD spectra for Co atoms lying respectively at $X = 4.6$, 1.8, and 0.4 ML from the interface. The spectra are normalized to the incident photon flux. Lowest panel: the three representative dichroic spectra normalized to the XMCD intensity at L_2.

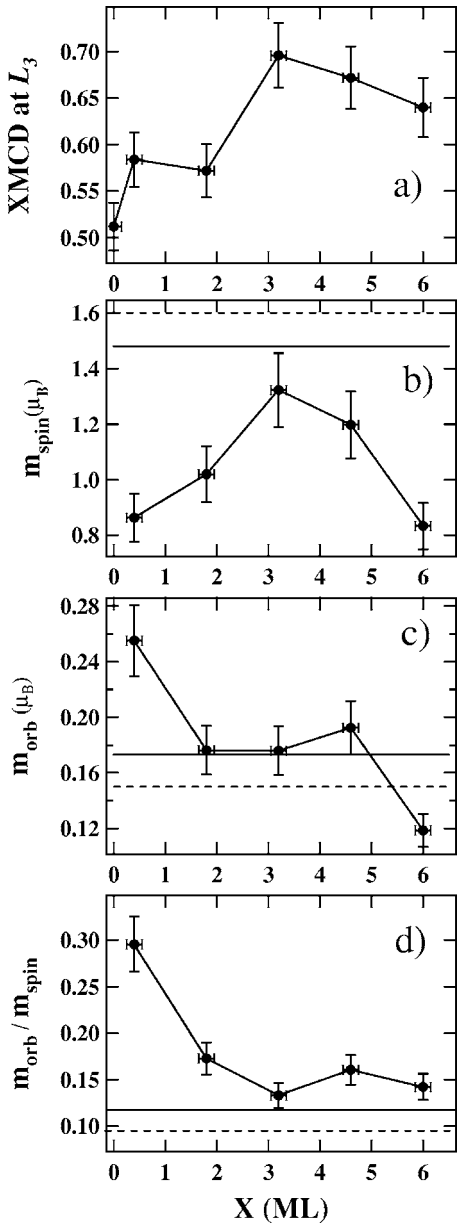

FIG. 5. Layer selective XMCD analysis. (a) The asymmetry intensity at Co L_3 edge. (b)–(c) Respectively the spin-and orbital-magnetic moments of Co atoms as calculated by means of the sum-rules. (d) The orbital-to-spin magnetic-moment ratio. X indicates the distance of Co atoms from the interface (cf. Fig. 1): $X=0$ represents Co atoms in direct contact with the GaAs and $X=6$ represent Co atoms lying at the surface of the Fe film. The continuous and dashed horizontal lines indicate reference values for Co hcp (Ref. 24) and FeCo bcc (our data) thick films. The data are corrected for the incomplete light polarization (75%) and for 45° incidence angle with respect to the magnetization direction.

tion in the vicinity of the interface. This is readily seen in Fig. 4(d) where the XMCD spectra relative to 4.6, 1.8, and 0.4 ML probing thicknesses are shown normalized to the Δ_2 intensity. Since the Δ_3 intensity increases for the spectra relative to Co atoms sitting closer to the FM/SC interface, from Eq. (1) it follows that the orbital moment within the Fe film increases when approaching the interface.

IV. DISCUSSIONS

The magnetic behavior of the system observed by MOKE is in good agreement with previous reported studies performed on the Fe/GaAs(001)-(4×6) interface,[4,5] in particular regarding the critical thickness of 3 ML for the onset of the FM state. Moreover, knowing that (i) the substrate diffraction pattern disappears at the thinnest Fe coverage, while a square pattern appears at nominal thickness of 3 ML, and (ii) the comparison between LEED results and MOKE loops vs. Fe thickness, we are able to confirm that as soon as the Fe islands start to coalesce into a continuous single-crystal film, the ferromagnetic phase sets in.[4–7,31] Keeping in mind that this parameter is strictly dependent upon substrate preparation and growth conditions, the use of a wedge-shaped sample guarantees a better reliability in the results. In the single-wedge samples, the remnant magnetization increases for increasing thickness and the highest value of the magnetization is found at the edge of the sample, whereas for the double wedge, the magnetization remains rather constant over the whole sample area. This feature is crucial for the validity of the XMCD analysis since it confirms that the sample is fully remnant magnetized. The trend of the Fe total magnetic moment—also plotted in Fig. 2(a)—closely resembles the one of the Kerr response over the entire sample area, confirming that the Kerr effect in transverse mode can be reliably used to probe the sample magnetization.

In Fig. 2(b) it can be seen that the onset of the FM state in the wedge-shaped samples is accompanied by the opening of the hysteresis loop. The behavior of the coercive field of the double wedge deserves a more accurate analysis. In fact the presence of a number of lattice defects in the present heteroepitaxial system would suggest that the magnetization reversal occurs through the domain walls rotation and motion. Such a phenomenon is normally hindered by the presence of pinning centers. The observed increase of the H_c in the center part of the sample can then be attributed to the presence of the double Fe-Co interface, where lattice defects and pinning centers are likely to be concentrated.

The XPS analysis of the samples reveals important features on the chemical profile of the Fe/GaAs interface. Firstly, the overall sample thickness is constant along the whole sample area and the Co atoms are spatially well confined within the two oppositely oriented Fe wedges [Fig. 3(c)]. That the Co sensing layer does not diffuse or intermix into Fe is also suggested from the fact that the Co $3p$ intensity remains constant through the whole wedge, as shown in Fig. 3(b). Secondly, looking at the evolution of the Fe $3p$ signal, we notice that starting from 3 ML the observed trend changes considerably [see Fig. 3(a)]. This can be taken as the fingerprint of the coalescence of the Fe islands:[32] by melting in a continuous film, the contribution of Fe atoms whose intensity was screened by the topmost atoms of the islands was increased. The reduction observed for the highest coverage is most probably due to the presence of substrate atoms segregating in the near-surface region. A similar conclusion was drawn in a previous study performed on thin Fe films of increasing thickness deposited on GaAs(001)-$c(8\times2)$, where the abundance of As in the surface region was confirmed by angular-dependent XPS.

The presence of a surface segregation has been *a posteriori* confirmed by low photon energy (<40 eV) ARPES experiments on the same sample, where the Fe layers did not display, in valence band spectra, any trace of carbon or oxygen contaminants for more than one day after the sample preparation, thus indicating the presence of a "protective" As layer.[33] Finally, some important details of the Ga and As segregation (diffusion) are revealed from the XPS spectra. The thickness-dependent core-level shift for Ga and As suggests that the two atomic species diffuse from the substrate along the Fe overlayer, occupying fcc interstitial sites in the metal matrix.[32] Recent first-principle density-functional calculations from Mirbt *et al.* support the segregation of both Ga and As through the Fe film;[13] As segregation is expected even at 0 K, whereas the one of Ga occurs in a diffusive way, thus preferring to disperse within the film rather than to localize at the interface. Moreover, Ga segregation towards the surface is inhibited if As is already present in the topmost layers. To address the issue of segregation, we can use our XPS data. For the clean substrate [upper spectrum of Fig. 3(a)] the ratio between As and Ga 3*d* peaks depends on the relative abundance of the substrate atoms in the surface region and on the relative photoionization cross sections. Both these parameters are difficult to assign due to the large errors introduced by the unknown values of surface sensitivity and cross sections in real systems. In order to evaluate the segregation dynamics as a function of the Fe film thickness, we have normalized to unity both As and Ga 3*d* intensities for the clean GaAs(001)-(4×6) surface. Although this may appear as an arbitrary assumption, it is justified when the relative amount of segregation is concerned. Turning the attention to the As-to-Ga ratio for increasing Fe thickness, our XPS data show that the diffusion rate of the Ga and As is uneven across the film. In fact, once the Fe islands have coalesced in a bcc structure at around 3 ML, the Ga diffusion rate is more pronounced up to a nominal thickness of 4 ML. For higher coverage the As segregation prevails, thus inhibiting further Ga migration to the surface and leading to the formation of the well-known As-rich Fe surface with Ga distributed within the film. It must be stressed that for the highest coverage, the XPS sampling depth in the Fe matrix is limited to a few ML as shown by the Co 3*p* attenuation depth [Fig. 3(c)].

The XMCD results from the Co sensing layer correspond to Co atoms evenly enveloped in a macroscopically magnetized Fe film, thus coordinated with Fe neighbors. The Co magnetic environment reflects the local magnetization of the Fe film and allows one to "profile" it from the interface up to the surface. We observe a net dichroic signal through the whole interface, including for Co atoms in direct contact with the substrate [Fig. 5(a)]. This evidence rules out the presence of a magnetically dead interface layer, in agreement with XMCD measurements performed on capped samples.[18] Nevertheless, from our set of data it is possible to follow the spin and orbital magnetic moments along the Fe film thickness in more detail and one observes that the spin-polarization is maximum at the center of the film and it decreases for smaller probing distances. A spin magnetic quenching is also observed for the layers closer to the Fe film surface. The reduction of the spin magnetic moment measured for the Co atoms in the vicinity of the interface can be explained as being due to the presence of As and Ga atoms segregating from the substrate. In fact, as pointed out by recent theoretical calculations,[13] at the earlier stages of adsorption of Fe on GaAs(001), the Fe atoms tend to break the top Ga-As bonds to create Fe-As bonds through 3*p*-3*d* hybridization, with Ga taking interstitial sites. Since the magnetic phase diagram of the thin film depends critically on the small details of the Fe electronic configuration, a change in the coordination and distance between Fe and segregating atoms can modify the Fe 3*d* states' delocalization and hinder the exchange interaction. Such a modification in the exchange force among the Fe atoms will result in a reduced magnetization at the interface with the SC as measured via the Co magnetic marker. Similarly, the presence of foreign atoms at the top of the Fe film, as detected by XPS, can explain the reduction of the measured spin-polarization at the surface of the sample.

It is interesting to note that reduction of the spin magnetic moment measured at the interface and at the film surface is somewhat smaller than expected. In fact, according to calculations, for Fe adsorption on GaAs(001), a complete quenching of the Fe magnetic moment should occur once the Fe-As distance reduces to a critical value of 2.36 Å and this situation is theoretically met at the interface also when the Fe film is 5 ML thick.[13] Remarkably, our data show that the magnetization, measured across the Co magnetic marker, does not vanish at any distance from the interface. Similarly, the almost complete quenching expected at the surface renormalizes to magnetization reduction in our experimental results. Both these discrepancies are probably due to the fact that the local chemistry is more complex than predicted theoretically due to the presence of the intermixing of different phases.

As shown in Fig. 5(c) the orbital moment measured for the Co atoms embedded in the bcc Fe film increases as approaching the interface. An increase of the orbital moment was also detected for the Fe atoms by XMCD in the recent work of Claydon *et al.*[18] For very thin layers of Fe buried beneath Co and/or Cr thick layers, the authors found an increased orbital moment for Fe thickness smaller than 12 ML with respect to the Fe bulk value while the orbital moment remained rather constant for thicknesses ranging from 8 ML down to submonolayers. Our data show a somehow different trend: the Co orbital moment increases sensibly across the 6 ML of Fe when approaching the interface with GaAs(001)-(4×6) and we measure an important variation of the orbital moment even between 6 and 4 ML. This apparent disagreement may be due to the different sample preparations. As pointed out by Claydon *et al.*, the presence of the heterogeneous interface may induce a localization of the Fe 3*d* orbitals leading to an increased atomiclike orbital moment. We would like to stress that the observed behavior is accompanied by a chemical heterogeneity of the film as detected by XPS. It is then likely that the presence of substrate segregating species along the film thickness may end up in a varying local chemical environment for the FM atoms. Consequently, the strong quenching of the orbital moment observed in a homogeneous single-crystal film[24] may be hindered even though the epitaxial bcc structure is preserved against segregation.

To reduce the uncertainty on the magnetic-moment value measured by the sum rules, one often refers to the ratio between the orbit and the spin moments, which is independent of final state electronic configuration and isotropic spectrum. The resulting ratio between the orbital and spin magnetic moment displayed in Fig. 5(d) shows an increased value with respect to Co hcp and FeCo bcc reference samples. This feature was already observed in thin Fe films on GaAs(001).[18,22,34] In the present study the overall increase is detected in more detail, showing that a stronger increase is due to the presence of the interface layers.

Finally, we would like to point out that the layer-sensitive evaluation of the orbital moment might play a key role in explaining the phenomenon of UMA observed in these systems. In fact, one of the possible routes to explain this phenomenon is the anisotropic bonding of Fe atoms with the twofold symmetric substrate: since the crystalline anisotropy is driven by the anisotropy of the spin-orbit interaction, a possible orbital moment anisotropy induced by the anisotropic bonding with substrate atoms would confirm the hypothesis mentioned above. The observed increase of the orbital moment can be a consequence of such anisotropy as observed in low-dimensional systems showing perpendicular magnetic anisotropy.[25,26] The present sensing layer technique with XMCD may give fruitful information on the way the anisotropy propagates within the film. Angular-dependent XMCD studies are on the way to further corroborate this hypothesis.

V. CONCLUSIONS

We reported on the magnetic and chemical properties of Fe thin films deposited *in situ* on GaAs(001)-(4×6). The use of a wedge-shape sample with a magnetic sensing layer allowed us to follow the growth and the magnetization onset in a continuous mode. In agreement with previous results, we found islands of Fe to coalesce into a continuum film at a nominal thickness of 3 ML. At the same time, the rate of segregation of the substrate atoms was found to be uneven with Ga prevailing between 3 and 4.5 ML (probably due to the Ga termination of the present reconstruction) while As segregation becomes more important at higher coverage. The Fe coalescence was accompanied by the onset of magnetization as observed by MOKE. Subsequently, by depositing 1 ML $Fe_{0.5}Co_{0.5}$ onto the Fe wedge and by covering this structure with an Fe counterwedge, we realized half a ML of Co embedded in an evenly thick Fe film. The MOKE measurements show that the magnetization was constant all through the sample. The observed increase of the coercive field at the center of the sample is interpreted as due to the presence of a double interface with a higher number of pinning centers for domain nucleation that hinder the magnetization reversal process.

A layer-sensitive study was then performed by employing the XMCD technique and by focusing the x-ray beam on Co atoms residing at different distances from the metal/semiconductor interface. The results can be summarized as follows: the dichroic signal persists even for Co atoms in direct contact with the substrate, ruling out the presence of a magnetically dead layer. The Co spin magnetic moment is maximum midway between the interface and the surface, where it is sensibly reduced. On the other hand, the orbital magnetic moment is found to increase when approaching the interface with GaAs, and it was interpreted as a consequence of the reduced local symmetry given by the presence of the interdiffusing substrate species. The orbit-to-spin magnetic-moment ratio is bigger with respect to Co hcp and FeCo bcc reference values, with the enhancement being greater for the layers closer to the interface.

Our results emphasize the importance of the chemical profile on the magnetic properties in this type of heteroepitaxial systems. It is worth noting that the sensing-layer approach was the key issue to probe the magnetic properties along the Fe film thickness. This method appears to be more reliable than a thickness-dependent analysis as far as the interface properties are concerned. Moreover, the possibility of studying samples prepared *in situ* circumvents the ambiguity introduced by the presence of a capping layer.

AKNOWLEDGMENTS

This work has been supported by EC, under Contract No. HPRI-CT-2001-50032 and by the Italian Minister of Internal Affairs. Special thanks are due to Professor G. Bayreuther for useful discussions.

[1] Igor Zutic, J. Fabian, and S. Das Sarma, Rev. Mod. Phys. **76**, 323 (2004).
[2] E. M. Kneedler, B. T. Jonker, P. M. Thibado, R. J. Wagner, B. V. Shanabrook, and L. J. Whitman, Phys. Rev. B **56**, 8163 (1997).
[3] A. T. Hanbicky, O. M. J. van't Erve, R. Magno, G. Kiosleoglou, C. H. Li, B. T. Jonker, G. Itskos, R. Mallroy, M. Yasar, and A. Petrou, Appl. Phys. Lett. **82**, 4092 (2003).
[4] Y. B. Xu, E. T. M. Kernohan, D. J. Freeland, A. Ercole, M. Tselepi, and J. A. C. Bland, Phys. Rev. B **58**, 890 (1998).
[5] F. Bensch, G. Garreau, R. Moosbuhler, G. Bayerheuther, and E. Beaurepaire, J. Appl. Phys. **89**, 7133 (2001).
[6] M. Madami, S. Tacchi, G. Carlotti, G. Gubbiotti, and R. L. Stamps, Phys. Rev. B **69**, 144408 (2004).
[7] S. J. Steinmuller, M. Tselepi, G. Wastlbauer, V. Strom, D. M. Gillingham, A. Ionescu, and J. A. C. Bland, Phys. Rev. B **70**, 024420 (2004).
[8] R. Moosbühler, F. Bensch, M. Dumm, and G. Bayreuther, J. Appl. Phys. **91**, 8757 (2002).
[9] M. Zölfl, M. Brockmann, M. Köhler, S. Kreuzer, T. Schweinböck, S. Miethaner, F. Bensch, and G. Bayreuther, J. Magn. Magn. Mater. **175**, 16 (1997).
[10] Y. Zhai, L. Shi, W. Zhang, Y. X. Xu, M. Lu, H. R. Zhai, W. X. Tang, X. F. Jin, Y. B. Xu, and J. A. C. Bland, J. Appl. Phys. **93**, 7622 (2003).

[11] S. C. Erwin, S.-H. Lee, and M. Scheffler, Phys. Rev. B **65**, 205422 (2002).
[12] I. Cabria, A. Ya. Perlov, and H. Ebert, Phys. Rev. B **63**, 104424 (2001).
[13] S. Mirbt, S. Sanyal, C. Isheden, and B. Johansson, Phys. Rev. B **67**, 155421 (2003).
[14] E. Sjöstedt, L. Nordström, F. Gustavsson, and O. Eriksson Phys. Rev. Lett. **89**, 267203 (2002).
[15] O. Thomas, Q. Shen, P. Schieffer, N. Tournerie, and B. Lépine, Phys. Rev. Lett. **90**, 017205 (2003).
[16] S. McPhail, C. M. Gürtler, F. Montaigne, Y. B. Xu, M. Tselepi, and J. A. C. Bland, Phys. Rev. B **67**, 024409 (2003).
[17] J. J. Krebs, B. T. Jonker, and G. A. Prinz, J. Appl. Phys. **61**, 2596 (1987).
[18] J. S. Claydon, Y. B. Xu, M. Tselepi, J. A. C. Bland, and G. van der Laan, Phys. Rev. Lett. **93**, 037206 (2004).
[19] http://ape.tasc.infm.it/
[20] M. Dumm, B. Uhl, M. Zölfl, W. Kipferl, and J. Bayreuther, J. Appl. Phys. **91**, 8763 (2002).
[21] M. Dumm, F. Bensch, R. Moosbühler, M. Zölfl, M. Brockmann, and G. Bayreuther, *Epitaxy and Magnetism of Fe and FeCo on GaAs(001): Growth, Onset of Ferromagnetism and Magnetic Anisotropies*, in NATO Advanced Study Institute on Magnetic Storage Systems Beyond 2000 (Kluwer Academic, Dordrecht, 2002), Vol. 41, p. 555.
[22] Y. B. Xu, M. Tselepi, C. M. Guertler, C. A. F. Vaz, G. Wastlbauer, J. A. C. Bland, E. Dudzik, and G. van der Laan, J. Appl. Phys. **89**, 7156 (2001).
[23] W. L. O'Brien and B. P. Tonner, Phys. Rev. B **50**, 12672 (1994).
[24] C. T. Chen, Y. U. Idzerda, H.-J. Lin, N. V. Smith, G. Meigs, E. Chaban, G. H. Ho, E. Pellegrin, and F. Sette, Phys. Rev. Lett. **75**, 152 (1995).
[25] P. Gambardella, A. Dallmeyer, K. Maiti, M. C. Malagoli, W. Eberhardt, K. Kern, and C. Carbone, Nature (London) **416**, 301 (2002).
[26] P. Gambardella, S. Rusponi, M. Veronese, S. S. Dhesi, C. Grazioli, A. Dallmeyer, I. Cabria, R. Zeller, P. H. Dederichs, K. Kern, C. Carbone, and H. Brune, Science **300**, 1130 (2003).
[27] L. Giovanelli, C.-S. Tian, P. L. Gastelois, G. Panaccione, M. Fabrizioli, M. Hochstrasser, M. Galaktionov, C. H. Back, and G. Rossi, Physica B **345**, 177 (2004).
[28] J. Stohr, J. Magn. Magn. Mater. **200**, 470 (1999).
[29] E. Di Fabrizio, G. Mazzone, C. Petrillo, and F. Sacchetti, Phys. Rev. B **40**, 9502 (1989).
[30] P. Ryan, R. P. Winarski, D. J. Keavney, J. W. Freeland, and R. A. Rosenberg, S. Park, C. M. Falco, Phys. Rev. B **69**, 054416 (2004).
[31] S. J. Steinmuller, M. Tselepi, V. Strom, and J. A. C. Bland, J. Appl. Phys. **91**, 8679 (2002).
[32] S. A. Chambers, F. Xu, H. W. Chen, I. M. Vitomirov, S. B. Anderson, and J. H. Weaver, Phys. Rev. B **34**, 6605 (1986).
[33] L. Giovanelli, G. Panaccione, M. Fabrizioli, A. Stollo, C. H. Back, and G. Rossi (unpublished).
[34] Y. B. Xu, M. Tselepi, E. Dudzik, C. M. Guertler, C. A. F. Vaz, G. Wastlbauer, D. J. Freeland, J. A.C. Bland, and G. van der Laan, J. Magn. Magn. Mater. **226**, 1643 (2001).